Photoexcitations in composites of poly(paraphenylene vinylene) and single-walled carbon nanotubes

J. Wéry, H. Aarab,* S. Lefrant, and E. Faulques
Laboratoire de Physique Cristalline, Institut des Matériaux Jean Rouxel, 2 rue de la Houssiniére, BP32229, F-44322 Nantes, France

E. Mulazzi and R. Perego
Dipartimento di Fisica, Universita' degli Studi di Milano, and Istituto Nazionale di Fisica della Materia Via Celoria 16, 20133 Milano, Italy

(Received 25 June 2002; revised manuscript received 3 December 2002; published 13 March 2003)

Absorption and photoluminescence (PL) studies have been carried out on pristine standard poly(paraphenylene vinylene) PPV and a series of PPV-single-walled carbon nanotubes (SWNT) composite films. Drastic changes in the PL and absorption spectra are observed with the increase of the SWNT fraction. A model is presented which is able to explain quantitatively the modification of absorption spectra, and particularly the new features in PL spectra as a function of SWNT percentages in the films. We provide evidence for strong electronic interaction between SWNT and the PPV polymer precursor precluding the complete thermal conversion of the polymer matrix.

DOI: 10.1103/PhysRevB.67.115202 PACS number(s): 78.40.Ri, 78.55.Kz, 78.66.Qn, 78.66.Sq

I. INTRODUCTION

Conjugated polymers belonging to the class of poly(paraphenylene-vinylene) PPV have been the subject of intensive research because of their photoluminescence (PL) properties in the visible range.[1] They have been used as light emitting diodes (LED) in devices.[2] It is expected that conjugation length in the PPV chains should influence both the absorption and emission spectra as it has already been shown.[3–5] On the other hand, nanotubes of carbon are materials with remarkable mechanical and electrical properties. In fact, the electronic properties of individual single-walled nanotubes (SWNT) strongly vary with tube diameter and chirality.[6,7] Polymer composites containing carbon nanotubes may thus be of considerable technological interest, because they may combine the best electrical, mechanical, and optical properties of each of the components. In this context, SWNT and multiwalled nanotubes have been dispersed in a number of different polymer matrices in order to achieve the elaboration of composites with enhanced electronic properties for layers in electronics or with new rheological behavior.[8–14] In these respects it seems very interesting to study the properties of combined SWNT and PPV, because such composites could be applied for several macroscopic devices such as tunable LED's. In fact novel electronic properties could be determined either by microscopic interactions between the polymer and SWNT or by varying the conjugation length distribution in the polymer chains.

In this work we report on absorption and PL properties of SWNT-PPV composites at different concentrations. By using a model based on the distribution of effective conjugation lengths in the polymer and their modifications as a function of the SWNT concentrations we present the calculated absorption and PL spectra for the same composite samples. We show that the optical properties of the composites are drastically affected by the change of the effective PPV conjugation length resulting from the filling of the polymer with SWNT.

II. EXPERIMENTAL DETAILS

Composites were obtained by mixing SWNT at different weight concentrations in the soluble sulfonium polyelectrolyte precursor of PPV with sonication and by depositing the solutions in an inert gas atmosphere at room temperature on quartz substrates. The samples were subsequently heated under vacuum at 300 °C to achieve the conversion of PPV polymer precursor.[15] Thin films with thicknesses of about 300 nm were obtained in this way. The absorption spectra of the films were recorded at room temperature (RT) by using a Cary5 UV-visible-near-infrared spectrometer working in transmission mode in the range 1.80 eV–6.60 eV. The PL spectra, also recorded at RT, were acquired in reflection geometry with a Jobin-Yvon Fluorolog spectrometer by using different excitation wavelengths.

III. RESULTS AND DISCUSSION

We show in Fig. 1 the optical absorption spectra of standard PPV and of composite films with concentrations of SWNT from $x=1\%$ to $x=64\%$ in weight of the precursor polymer, in the energy range of 1.8–3.6 eV. In order to better compare Figs. 1(a)–1(e), we have taken the same baseline in the low-energy side, i.e., at 2.1 eV. We can verify that the broad absorption band of standard PPV [Fig. 1(a)] due to the $\pi \rightarrow \pi^*$ electronic transition in this energy region is very similar to that published elsewhere at RT.[4] Moreover, we observe that this band broadens, and gradually decreases in intensity when x increases. In addition, we can deduce from a careful analysis that this band exhibits also a small blue shift. These significant features on the absorption of composite films clearly indicate that the effective conjugation length in these films becomes shorter with respect to standard PPV when the concentration of SWNT in the samples increases.[4]

In order to understand better the role of SWNT in composite films, we present in Fig. 2 the optical absorption spectra of standard PPV and of composite films in the energy

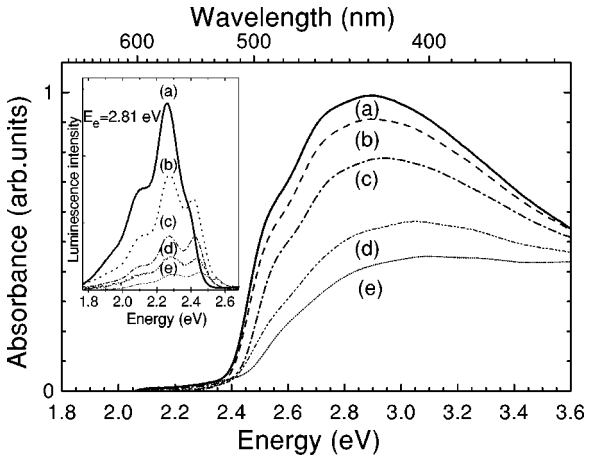

FIG. 1. Optical absorption at room temperature of standard PPV and PPV-SWNT composites for different SWNT weight percentages *x*. (a) standard PPV, (b) $x=1\%$, (c) $x=16\%$, (d) $x=32\%$, (e) $x=64\%$. Spectral range, 1.8–3.6 eV. The inset shows the photoluminescence (emission) spectra of standard PPV (solid bold line) and several composites for the 2.81-eV excitation energy (thin lines, dashed). The PL intensity diminishes when the SWNT concentration increases.

region between 3.0 eV and 6.6 eV. In Fig. 2(a) (PPV), two main bands are clearly observed at 4.7 eV and 6.0 eV. These bands have been extensively discussed recently and it comes out from literature[16–18] that they are assigned to intrinsic transitions of PPV, namely, to charge-transfer transitions between localized and delocalized levels ($l\rightarrow d^*$ and $d\rightarrow l^*$), and $l\rightarrow l^*$, respectively. The presence of another reported band at 3.7 eV attributed to the $d\rightarrow d^*$ transition is also presumably present in curve (a) on the high-energy side of the $\pi\rightarrow\pi^*$ transition band. Several observations can be made on these bands in composites when the concentration *x* of SWNT increases. On one hand, their intensity increases, and on the other hand, the 4.7 eV and 6.0 eV bands shift to 5 eV and 6.2 eV, respectively. This behavior can be interpreted as

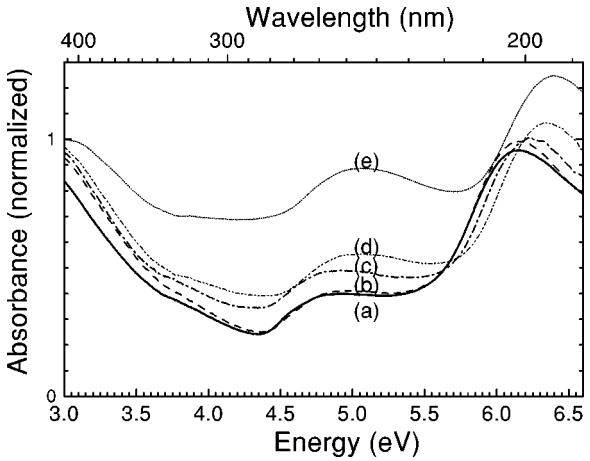

FIG. 2. Optical absorption at room temperature of standard PPV and PPV-SWNT composites for different SWNT weight percentages *x*. (a) standard PPV, (b) $x=1\%$, (c) $x=16\%$, (d) $x=32\%$, (e) $x=64\%$. Spectral range, 3.0–6.6 eV.

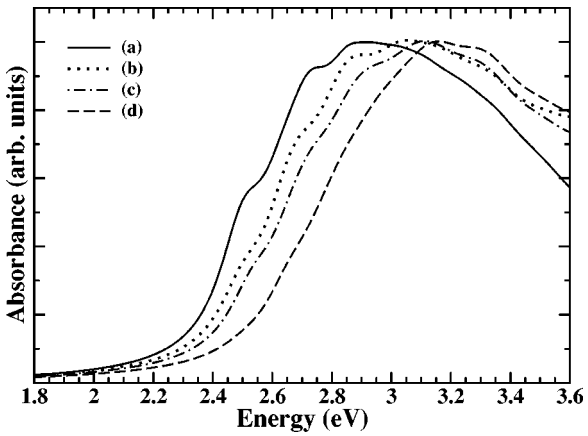

FIG. 3. Calculated optical absorption spectra at RT of standard PPV and PPV-SWNT composite films for different weight percentages *x*, (a) standard PPV, (b) 1% , (c) 16%, and 32%. All the bands have been normalized to the $\pi-\pi^*$ band of PPV.

due to a general decrease of the conjugation length of PPV corroborated by an apparent increase of the 3.7 eV component, if one refers to Ref. 17. Moreover, one cannot rule out the possibility of remaining tetrahydrothiophenium groups, or precursor, as it is observed in photoconverted PPV.[19–21] Both effects contribute to a shift of these two bands by adding contributions at higher energies, namely 5.35 eV and 6.2 eV. This is consistent with the fact that the conversion process is gradually inhibited when *x* increases. In other words, the presence of SWNT in composite films progressively prevents the complete conversion process of the PPV precursor polymer.[4,20]

In the inset of Fig. 1, we show the PL spectra at the excitation energy $E_{exc}=2.81$ eV (440 nm) for different *x* values. We note that, by increasing the SWNT percentage, a quenching of the PL is observed. This is due to a decrease in the absorbance of the main band, caused by the partial conversion of the precursor polymer as discussed above, and also by the charge transfer from conjugated PPV segments to the SWNT. We would like to point out that both effects are relevant to the high PL quenching and that preliminary photoconductivity results on these samples lead to this conclusion. In fact the photoconductivity increases dramatically with increasing *x*.[22] The more relevant feature in the PL spectrum shown in the figure is related to the increase of the intensity of the bump at 2.43 eV (510 nm), starting from $x=1\%$, which actually becomes a dominant peak in the spectrum as the *x* percentage increases.

In Fig. 3, we show the calculated absorption spectra at room temperature of standard PPV [Fig. 3(a)] and of the composite films with different *x* from 1% to 32%, in the energy range 1.8 eV–3.6 eV. The calculations have been performed by using the model presented in Ref. 4 and all the values are reported in Table I for the effective conjugation lengths with $n=2-10$. In this model the absorption band shape of PPV is calculated by considering the contribution of the absorption band for effective conjugation lengths from $n=2$ to $n=10$ weighted by a distribution P_n. P_n simulates the distribution of effective conjugation lengths which can be found statistically over the entire polymer part of the com-

TABLE I. Values of Ω_n, $S_{f,n}$, and γ_n, used for the calculations of absorption band shapes of different PPV and PPV-SWNT samples.

n	2	3	4	5	6	7–10
Ω_n(eV)	3.78	3.25	3.00	2.86	2.75	2.60
$S_{1,n}$	0.40	0.40	0.42	0.45	0.50	0.52
$S_{2,n}$	0.10	0.08	0.08	0.08	0.08	0.08
$S_{3,n}$	0.12	0.12	0.12	0.15	0.20	0.20
$S_{4,n}$	0.96	0.95	0.92	0.92	0.75	0.70
$S_{5,n}$	0.32	0.25	0.23	0.15	0.15	0.10
γ_n(eV)	0.12	0.12	0.14	0.16	0.18	0.20

posite. For the sake of clarity we give in the following the expression of P_n:

$$P_n = \frac{1-G}{(2\pi\sigma_1)^{1/2}} \exp - \left(\frac{n-n_1}{\sqrt{2}\sigma_1} \right)^2 + \frac{G}{(2\pi\sigma_2)^{1/2}} \times \exp - \left(\frac{n-n_2}{\sqrt{2}\sigma_2} \right)^2, \quad (1)$$

where n_1 and σ_1 are the mean value of the segment lengths and the standard deviation, respectively, of the distribution for $n=2-6$, n_2 and σ_2 are the parameters of the distribution for $n=7-10$, and G is the weight of the second distribution relative to the first one. By considering the values of the electronic transitions Ω_n, the electron-vibration coupling $S_{f,n}$ ($f=1-5$ numbers in the vibrational modes) and γ_n given in Table I for the absorption together with the parameters given in Table II, we have calculated the absorption band shapes for $x=0\%$, 1%, 16%, and 32% shown in Fig. 3. Note that the distribution parameters show an increase of the weight of the short segments going from $x=0\%$ to $x=32\%$. In the frequency range reported in the figure, a very good agreement is found between the calculated spectra and the experimental data of Fig. 1, for the different x concentrations, concerning both the shape and the blueshift of the bands. This proves that an increase of the percentage x in the composite films induces a real augmentation of the short segment contribution, as if the conversion temperature was lowered.

TABLE II. Distribution parameters used in the calculations of optical absorption spectra and PL spectra given in Figs. 3 and 5 of standard PPV and PPV-SWNT composite films for different weight percentages x from 0.5% to 64%. Standard PPV is indicated with $x=0$.

x	n_1	σ_1	n_2	σ_2	G
0	3	1	8	2	0.3
0.5	3	1	7	2	0.26
1	2	1	6	1	0.2
2	2	1	5	1.4	0.3
16	2	1	5	1.2	0.29
32	2	1	5	0.9	0.22
64	2	1	5	0.7	0.21

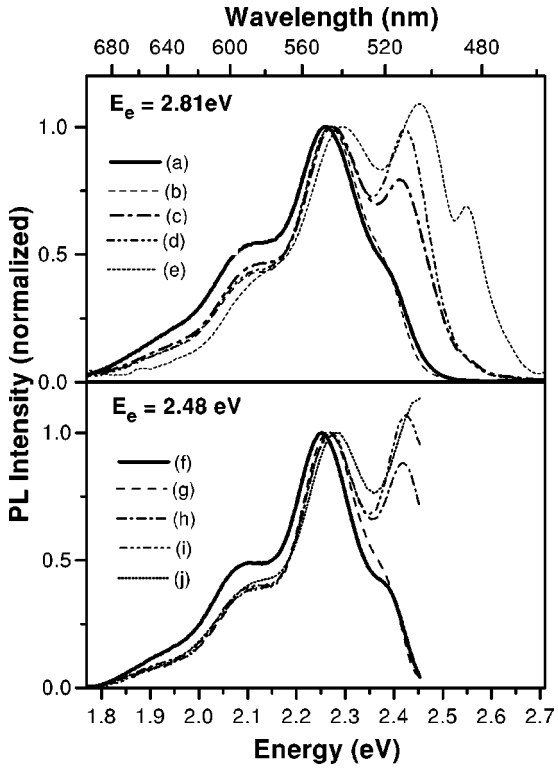

FIG. 4. Photoluminescence (emission) spectra at RT of standard PPV and PPV-SWNT composites for different SWNT weight percentages x. Excitation energy 2.81 eV, (a) standard PPV, (b) $x=0.5\%$, (c) $x=2\%$, (d) $x=16\%$, (e) $x=64\%$. Excitation energy 2.48 eV, (f) standard PPV, (g) $x=0.5\%$, (h) $x=2\%$, (i) $x=16\%$, (j) $x=32\%$. All the bands are normalized to the peak at 2.23 eV.

In Fig. 4, we show the PL spectra at $E_{exc}=2.48$ eV (500 nm) and $E_{exc}=2.81$ eV (440 nm), respectively, from PPV and composite films with different SWNT percentages. The PL spectra shown in Figs. 4(a)–(e) recorded for $E_{exc}=2.81$ eV are given for PPV and composite films with different $x=0.5\%$, 2%, 16%, 64%. The PL spectra shown in Figs. 4(a) and 4(b) are very similar indicating that only small changes in the samples are produced for $x=0.5\%$. The spectra consist of a principal peak at 2.23 eV (550 nm), a vibronic replica at 2.12 eV (575 nm), and a small bump at 2.43 eV. On the other hand starting from $x=1\%$ (not shown in the figure) the PL spectra undergo significant changes and the intensity of the band peak at 2.43 eV increases as the fraction x raises. We note that the vibronic replica at 2.12 eV (575 nm), still present in all the spectra, decreases in intensity as a function of x. In Fig. 4(e) we would like to call attention to a very remarkable spectral feature at 2.57 eV (482 nm). This new band can be observed only for this value of x. This band peak is at the same frequency position as the most intense feature in the PL spectrum of t,t distyrylbenzene in KBr (a three-ring PPV oligomer), reported in Fig. 4 of Ref. 23. In Figs. 4(f)–(j) the PL spectra are recorded for $E_{exc}=2.48$ eV for PPV and the composite film with $x=0.5\%$, 2%, 16%, and 32%. The PL spectra shown in Figs.

4(f) and 4(g) are very similar and almost equal to those shown in Figs. 4(a) and 4(b). Indeed, it is obvious from Figs. 4(h)–4(j) that the bands located at 2.23 eV and around 2.43 eV become very prominent features of the PL spectra. By increasing the SWNT concentration from 2% to 32%, the band at 2.23 eV slightly upshifts by about 10^{-2} eV. Note that the intensity of the band at 2.43 eV is overestimated, due to the excitation wavelength contribution in this energy range.

In order to calculate the photoluminescence spectra recorded for different SWNT concentrations in the composite films, we have to take into account the active mechanisms for energy transfer from short conjugated segments to the longer conjugated segments: the short-range and the long-range (Förster type) migration of the excitations. This last mechanism, through dipole-dipole interactions, favors the energy transfer from short to longer segments in one step. On the contrary, the short-range migration of the excitations between segments crucially depends on their interchain and intrachain dynamics, and therefore on the traps and defects (chemical and structural) which can prevent the complete energy transfer on the longest segments in the sample. As a consequence of these effects, the onset of the emission spectrum depends on (i) how effective the excitation migration process is in the different samples and (ii) on the excitation wavelengths.

Taking into account all these effects, and trying to simulate them, we have performed the calculation of the photoluminescence spectra by using the following equation:

$$I(\Omega)_{PL} = \sum_{n=n^*}^{10} I(\Omega,n)_{PL} P_n, \tag{2}$$

P_n is the distribution defined in Eq. (1) and used in the present calculations for the calculated absorption band shapes given in Fig. 3; n^* is the number of phenyl rings in the conjugation length of the shorter excited segments from which the radiative recombination begins; n^* depends both on the excitation energy E_{exc} and on the efficiency of the energy migration process. We recall that P_n simulates the distribution of effective conjugation lengths which are present on average in all the polymeric chains. We point out that in Eq. (2) the summation begins from n^* and not from 2 as in the case of absorption. Thus, the contribution of P_n to Eq. (2) in the PL process is substantially different from that calculated for the absorption. In this way, we simulate the excitation migration in the samples and relate the value of n^* to the excitation energy E_{exc} and to the sample through P_n, taking into account the traps and defects, which can prevent the energy migration to longer segments.

Therefore, in the present calculations, the onset of the photoluminescence spectrum and the intensity of the structures at higher energies both depend on the electronic energy value related to the segment length determined by n^* and on P_n. $I(\Omega,n)_{PL}$ is given in the following equation:

TABLE III. Values of $\Omega_{n,e}$, $S^e_{f,n}$, and $\gamma_{n,e}$ used in Eqs. (2) and (3) for the calculation of the emission spectra for different E_{exc} given in Fig. 5.

n	2	3	4	5	6	7–10
$\Omega_{n,e}$(eV)	3.51	2.82	2.54	2.44	2.31	2.26
$S^e_{1,n}$	0.14	0.14	0.15	0.16	0.16	0.16
$S^e_{2,n}$	0.06	0.06	0.06	0.06	0.06	0.06
$S^e_{3,n}$	0.07	0.07	0.08	0.10	0.11	0.12
$S^e_{4,n}$	0.78	0.62	0.57	0.50	0.42	0.34
$S^e_{5,n}$	0.15	0.11	0.11	0.10	0.10	0.07
$\gamma_{n,e}$(eV)	0.05	0.05	0.06	0.06	0.07	0.07

$$I(\Omega,n)_{PL} = |M_n|^2 \left\{ \sum_{j=0}^{2} \sum_{f=1}^{5} \exp\left[-\sum_{f=1}^{5} S^e_{f,n} \right] \frac{(S^e_{f,n})^j}{j!} \times \frac{\gamma_n}{(\Omega - \Omega_{n,e} + j\omega_f)^2 + \gamma^2_{n,e}} \right\}, \tag{3}$$

where M_n, $\Omega_{n,e}$, and $\gamma_{n,e}$ are the electric dipole moments, the electronic transition energy for the emission process, and the related width, respectively, for each segment whose length is determined by n. ω_f and $S^e_{f,n}$ are the frequencies of the stretching vibrations ($f=1-5$) and the electron vibration couplings in the final state in the emission process. j numbers the vibronic processes up to the second order for each vibration considered. In these calculations we use the same values for M_n, and ω_f as introduced in Ref. 4 for the absorption process, while $\Omega_{n,e}$, $S^e_{f,n}$, and $\gamma_{n,e}$, relative to the emission process, are given in Table III. All the values considered in the present paper are at room temperature. Note that the values of $\Omega_{n,e}$ are significantly lower compared to the values of the emission transitions of the isolated oligomers, following Ref. 24. Also $S^e_{f,n}$, according to the same arguments, are decreased with respect to the values of the electron-vibration couplings used for the absorption in the present paper as well as in Ref. 4. For the PL spectra of our PPV samples we define the following correspondence between n^* and E_{exc}:

$$\begin{aligned} &n^* = 4-5 \quad \text{for} \quad E_{exc} \geqslant 2.70 \text{ eV}; \\ &n^* = 6-7 \quad \text{for} \quad E_{exc} \simeq 2.50 \text{ eV}; \\ \text{and} \quad &n^* = 7 \quad \text{for} \quad E_{exc} \leqslant 2.41 \text{ eV}. \end{aligned} \tag{4}$$

The choice of this correspondence for n^* and E_{exc} is determined by the near resonance condition between the electronic transitions of the conjugated segments of length n^* and the excitation energy. Moreover, the choice between the two different values of n^*, for a given E_{exc}, depends on the interchain and intrachain dynamics of the excitations, which are strongly sample dependent.

In Fig. 5 we show the calculated photoluminescence spectra for $E_{exc}=2.81$ eV and $E_{exc}=2.48$ eV, respectively. In particular in Figs. 5(a)–5(e), we give the calculated PL spectra of standard PPV and the composite films with 0.5%, 2%, 16%, and 64% of SWNT for $E_{exc}=2.81$ eV, respectively. In

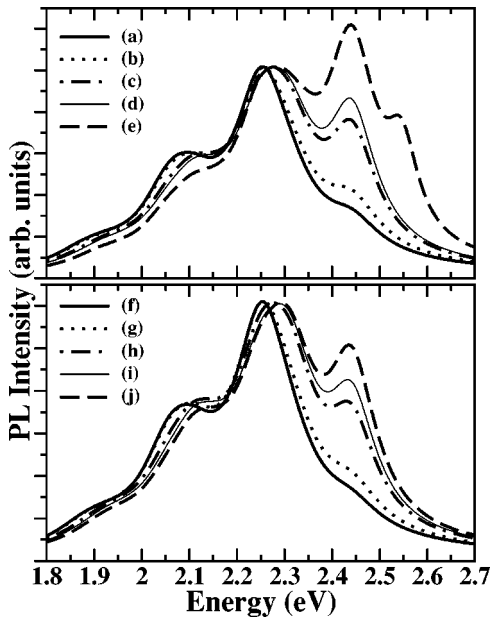

FIG. 5. Calculated PL spectra at RT of standard PPV and PPV-SWNT composite films for different SWNT weight percentages x. Excitation energy 2.81 eV, (a) standard PPV, (b) $x=0.5\%$, (c) $x=2\%$, (d) $x=16\%$, and (e) $x=64\%$. Excitation energy 2.48 eV, (f) standard PPV, (g) $x=0.5\%$, (h) $x=2\%$, (i) $x=16\%$, and (j) $x=32\%$. All the bands are normalized to the peak at 2.23 eV.

Figs. 5(f)–5(j), the calculated PL spectra of standard PPV and composite films with 0.5%, 2%, 16%, and 32% of SWNT, respectively, are displayed for $E_{exc}=2.48$ eV. All the spectra have been evaluated by using the correspondences given in Ref. 4; more precisely for the spectrum of Fig. 5(e) the sum in Eq. (2) was from 4 to 10, while for the spectra of Fig. 5(a)–5(d) the sum was from 5 to 10. Because of this difference a new peak at 2.57 eV, due to the conjugated segments whose effective length n is 4, arises in the PL spectrum for the composite films with $x=64\%$. The frequency position and the intensity of this structure are in very good agreement with those found in the experimental data of Fig. 4(e). From the discussion given before, this proves that in this kind of sample, defects and traps pin the excitations in the short segments. Moreover the PL spectra for $E_{exc}=2.48$ eV have been calculated by including 50% of the contribution of the segments with $n=5$, in the sum from 6 to 10 in order to have a better fit with the experimental data. This is an additional proof that the intrachain and interchain dynamics in the short-range excitation migration strongly depends on the sample, through the defects and traps which prevent the complete transfer of energy to the segments of longer conjugation. In fact in other PPV samples, whose PL spectra are given in Ref. 5, for $E_{exc}=2.48$ eV the contribution of conjugation lengths with $n=5$ disappears, indicating that the energy transfer to longer conjugated segments has been accomplished. From the calculated spectra given in Fig. 5, we can conclude that the peak at 2.43 eV is due to the pure electronic emission transitions of $n=5$ conjugated segments, while the peak at 2.23 eV corresponds to $n=7-10$ effective lengths. The other structures at 2.1 eV and 1.9 eV are the vibronic replica of first order and second order, respectively of the peak at 2.23 eV. Below the pure electronic transition peaks at 2.23 eV and 2.43 eV, there is also some contribution of the vibronic replica of the peaks at 2.43 eV and 2.57 eV, respectively.

IV. CONCLUSION

In summary, we have demonstrated that introducing nanotubes in PPV precursor solutions prevents the total conversion of the polymer when thermodynamical conditions such as time and annealing temperature are equivalent to those of standard PPV thermal conversion. In the early stages of the synthesis, the removal of the sulfonium salt is incomplete because of the presence of SWNT and the development of C=C double bonds along the polymer backbone is severely limited. Therefore, SWNT must strongly interact with the precursor at even low weight percentages. This process is definitely analogous to an accelerated aginglike transformation of the precursor whose efficiency and conversion yield are controlled by the nanotube concentrations. As a consequence, the blueshift of the main absorption band, the decrease in absorbance and the changes in the PL spectra are well explained with the model introduced here. In this approach, the modification of these features are determined by the formation of short segments, whose relative weight dominates over longer segments due to the addition of SWNT in the polymer precursor solutions. In conclusion, the presence of nanotubes as filler network in PPV may be of importance in view of applications, since it is possible to monitor the blue emission of the samples via a proper choice of the SWNT percentage in the films. Finally, we remark that the experimental and theoretical investigations, of the absorption and PL spectra of PPV-SWNT composite films presented here give a complete and accurate survey of their optical properties.

ACKNOWLEDGMENTS

The authors acknowledge G. Jonusauskas for experimental help. The Institut des Matériaux Jean Rouxel is Unité Mixte de Recherche No. 6502 au CNRS-Université de Nantes.

*Permanent address: Laboratoire de Physique du Solide, Faculté des Sciences Dher Elmahraz, B.P. 1796, Fès, Morocco.

[1] D.D.C. Bradley, R.H. Friend, H. Lindenberger, and S. Roth, Polymer **27**, 1706 (1986).

[2] J.H. Burroughes, D.D.C. Bradley, A.R. Brown, R.N. Marks, K. Mackay, R.H. Friend, P.L. Burns, and A.B. Holmes, Nature (London) **347**, 539 (1990).

[3] M. Jandke, Adv. Mater. **11**, 1518 (1999).

[4] E. Mulazzi, A. Ripamonti, J. Wéry, B. Dulieu, and S. Lefrant, Phys. Rev. B **60**, 16 519 (1999).

[5] E. Mulazzi, C. Botta, D. E. Facchinetti, and A. Bolognesi, Phys. Rev. B. (to be published).

[6] N. Hamada, S. Sawada, and A. Oshiyama, Phys. Rev. Lett. **68**, 1579 (1992).

[7] R. Saito, M. Fujita, G. Dresselhaus, and M.S. Dresselhaus, Phys. Rev. B **46**, 1804 (1992).
[8] E.T. Thostenson, Z. Ren, and T-W. Chu, Compos. Sci. Technol. **61**, 1899 (2001).
[9] P. Pötschke, T.D. Fornes, and D.R. Paul, Polymer **43**, 3247 (2002).
[10] E. Kymakis, I. Alexandrou, and G.A.J. Amaratunga, Synth. Met. **127**, 59 (2002).
[11] K. Jurewicz, S. Delpeux, V. Bertagna, F. Béguin, and E. Frackowiak, Chem. Phys. Lett. **347**, 36 (2001).
[12] H. Ago, M.S.P. Shafer, D.S. Ginger, A.H. Windle, and R.H. Friend, Phys. Rev. B **61**, 2286 (2000).
[13] S. Curran, P.M. Ajayan, W.J. Blau, D.L. Carroll, J.N. Coleman, A.B. Dalton, A.P. Davey, A. Drury, B. McCarthy, S. Maier, and A. Stevens, Adv. Mater. **10**, 1091 (1998).
[14] B. McCarthy, A.B. Dalton, J.N. Coleman, H.J. Byrne, P. Bernier, and W.J. Blau, Chem. Phys. Lett. **350**, 27 (2001).
[15] J.D. Stenger-Smith, R.W. Lenz, and G. Wegner, Polymer **30**, 1048 (1989).
[16] D. Comoretto, G. Dellepiane, D. Moses, J. Cornil, D.A. dos Santos, and J.L. Brédas, Chem. Phys. Lett. **289**, 1 (1998).
[17] D. Comoretto, G. Dellepiane, J.L. Brédas, J. Cornil, D.A. dos Santos, and D. Moses, Phys. Rev. B **62**, 10 173 (2000).
[18] E.K. Miller, D. Yoshida, C.Y. Yang, and A.J. Heeger, Phys. Rev. B **59**, 4661 (1999).
[19] J. Obrzut and F.E. Karasz, J. Chem. Phys. **87**, 2349 (1987).
[20] J. Bullot, B. Dulieu, and S. Lefrant, Synth. Met. **61**, 211 (1993).
[21] J. Wéry, B. Dulieu, J. Bullot, M. Baitoul, P. Deniard, and J.P. Buisson, Polymer **40**, 519 (1999).
[22] J. Wéry, L. Mihut, H. Aarab, S. Lefrant, E. Faulques, R. Perego, and E. Mulazzi (unpublished).
[23] N.F. Colaneri, D.D.C. Bradley, R.H. Friend, P.L. Burn, A.B. Holmes, and C.W. Spangler, Phys. Rev. B **42**, 11 670 (1990).
[24] J. Cornil, A.J. Heeger, and J.L. Brédas, Chem. Phys. Lett. **272**, 463 (1997).